12th IEA Heat Pump Conference 2017

Study on the Frosting Phenomena between Concavity and Convexity Plate under Forced Convection

-Detailed Observation and Analysis of Frost Layer Grouth-

Kenzo YASUI[**], Masafumi KATSUTA[*], Hiroki DOSHIDA[**], Ryo MIYAHARA[**]

[*]*Department of Modern Mechanical Engineering, Waseda University, Shinjuku-ku, Tokyo, 169-8555, Japan*
[**]*Graduate School of Environment and Energy Engineering, Waseda University, Shinjuku-ku, Tokyo, 169-8555, Japan*

Abstract

Currently, the development of hybrid and electric vehicles has been promoted. Along with this, since the impact reduction for cruising distance and the securing of the heat source are problems, changes are also required for the air conditioner. Therefore, high efficiency of the air conditioning system by improving efficiency of the heat exchanger and changing to heat pump system has become more and more necessary. However, due to frost formation of the outside heat exchanger by the use of a cold climate region, increase of pressure drop and decrease of heat transfer rate are expected to be an application difficulty of HP systems.

The objective of this study is to analyse the mechanism of frosting phenomenon in fin-less heat exchanger. This is intended to clarify the advantage in terms of frost strength and defrosting performance fin-less heat exchanger for the future candidate of heat exchanger.

We investigate basic characteristic of frost formation of the flow path between flat plate with concavity and convexity under forced convection. Test section is a flow path that is placed opposite to a flat plate having a periodic concavity and convexity groove on the surface. By using microscope and high speed VTR, we achieved a visualization of overall test section and observation of frost layer growth and frost formation are analysed by using of the VTR image. Finally, the relation between duration until incipient passage blockage and channels geometry becomes clear.

Keywords: Frosting Phenomena under Convection, Frost Layer Growth, Finless Heat Exchanger

1. INTRODUCTION

Currently, as a power train alternative to gasoline and diesel vehicles in the automotive industry, the development of hybrid and electric vehicles has been promoted. Along with this, since the impact reduction for cruising distance and the securing of the heat source are problems, changes are also required for the air conditioner. Therefore, high efficiency of the air conditioning system by improving efficiency of the heat exchanger and changing to heat pump system has become more and more necessary. However, due to frost formation of the outside heat exchanger by using in the cold climate region, increase of pressure drop and decrease of heat transfer rate are expected to be a problem on HP systems.

Multi-flow type heat exchanger having a corrugated-louvered fin is the mainstream of the heat exchanger for a vehicle, and the fin and tube miniaturization has been progressing in order to improve the performance. Thereby, since the retention amount of the condensed water or melting water between the fins increases, frost strength and defrosting performance is feared to be reduced. As improved method for these problems, fin-less type heat exchanger has been proposed to prevent the retention of condensate. This study is to analyse the mechanism of frosting phenomenon in fin-less heat exchanger, it is intended to clarify the advantage in terms of frost strength and defrosting performance fin-less heat exchanger for the current heat exchanger.

1. METHODOLOGY

2.1. Experimental Apparatus

Fig.1 is a schematic diagram of experimental apparatus. Experimental apparatus is composed of constant temperature and humidity air chamber, blower, orifice flow meter, test section and the duct. The air controlled temperature and humidity by the chamber, is flowing into the test section by the blower and then returned to the chamber. Air temperature and humidity before and after the test section was measured by thermocouples and humidity sensors. In addition to the area of frost layer, diameter and interval distance of crystal columns were measured by using an image processing.

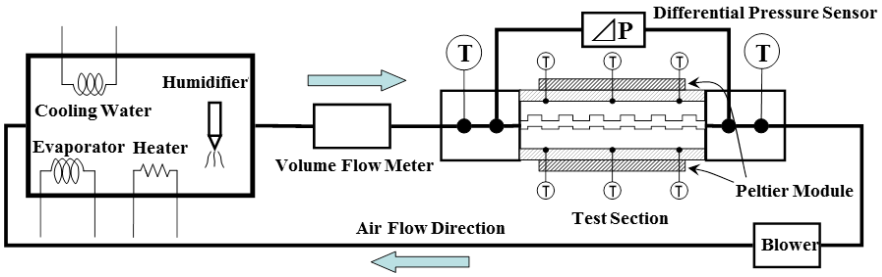


Fig. 1. Schematic of Experimental Apparatus

2.2. Test Section

Fin-less heat exchanger has a shape like Fig.2. In this study, we focus on the air side passage, and prepare the test section single out flow channel as shown in Fig.3. Test section has a periodic convex-concave shape as shown in Fig.4, and the size of each part is defined as shown in Fig.5.

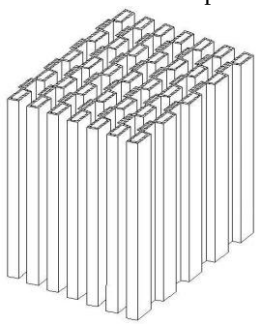


Fig. 2. General View of Heat Exchanger

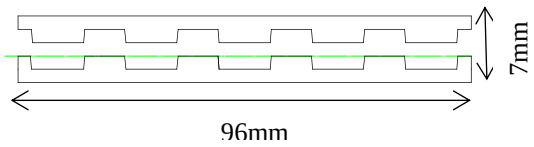


Fig. 4. Flow Channel of Test Section

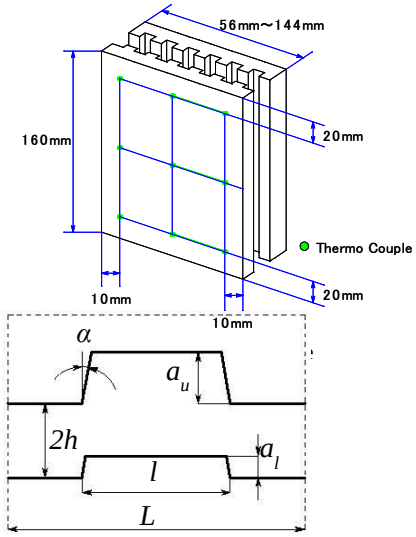


Fig. 5. Detail of Flow Channel

2.3 Experimental methodology and condition

First, air conditions in the chamber were adjusted to the experimental aimed value as shown in table 1. Turn off the blower after confirmation of the steady state, and the test section was cooled down to a set temperature. The experiment started after reaching the set temperature, and to measure the temperature, humidity and pressure drop across the test section until channel blockage, and the state of frost growth was taken by camera. Then, the test section was removed, and frost weight was measured. Air flow rate decreases in accordance with frost growth, however the blower output was fixed. Design parameters of test section are shown in Table 2.

After the end of each experiment, the height of the frost layer was taken by camera from the top of test section, and the height of the frost layer was measured. The captured image can be incorporated into image processing and analysis software, and then the height of frost layer is measured.

Table 1. Experimental Conditions

Inlet Air Temperature T_a	℃	7.0
Inlet Absolute Humidity X_a	kg/kg'	0.00533
Cooling Surface Temperature T_w	℃	-10.0
Initial Air Volume	m^3/h	5.0



Fig. 6. Frost Layer Image

Table 2. Design Parameters of Test Section

			No.1	No.2	No.3
Height of Convexity Portion	a_l	mm	2.0	1.2	2.8
Depth of Concavity Portion	a_u	mm		2.8	
Length of convex-concave portion	l	mm		8.0	
Pitch of convex-concave	L	mm		16.0	
Taper Angle of Unevenness	α	Deg		10	
Number of convex-concave	N	-		6	
Interval of Plate	-	mm		4	

3. RESULTS AND DISUCUSSION

3.1. Area of frost layer

Test pieces are named as Upper and Lower side, respectively as shown in Fig. 7. Area of the frost layer is measured from captured image taking from the top of test section.

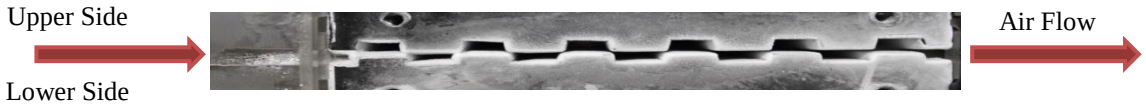


Fig. 7. Area of frost layer

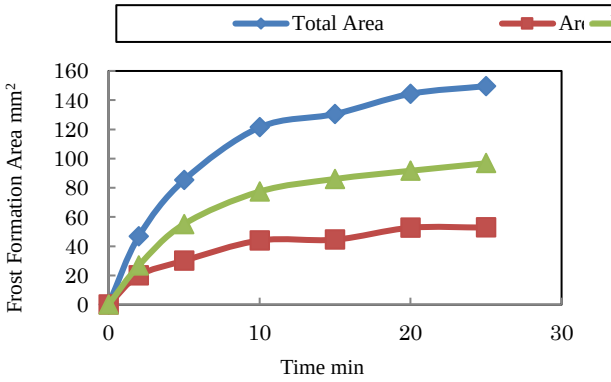


Fig. 8. Frost Formation Area (No.1)

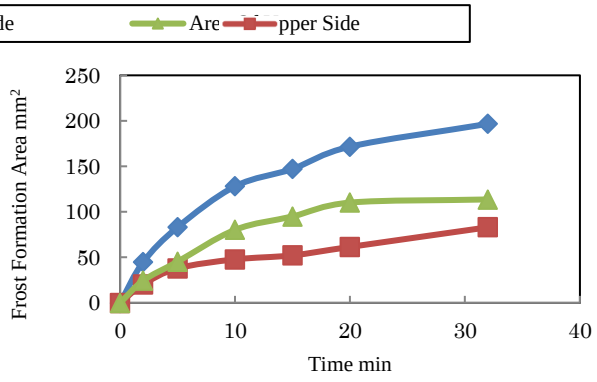


Fig. 9. Frost Formation Area (No.2)

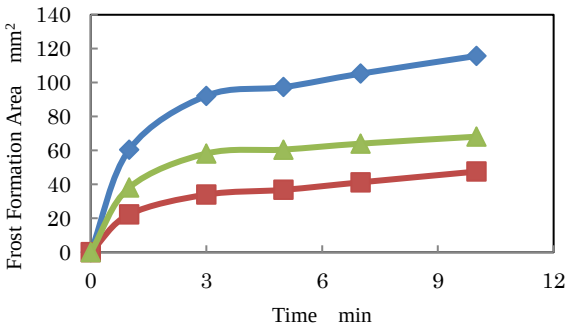
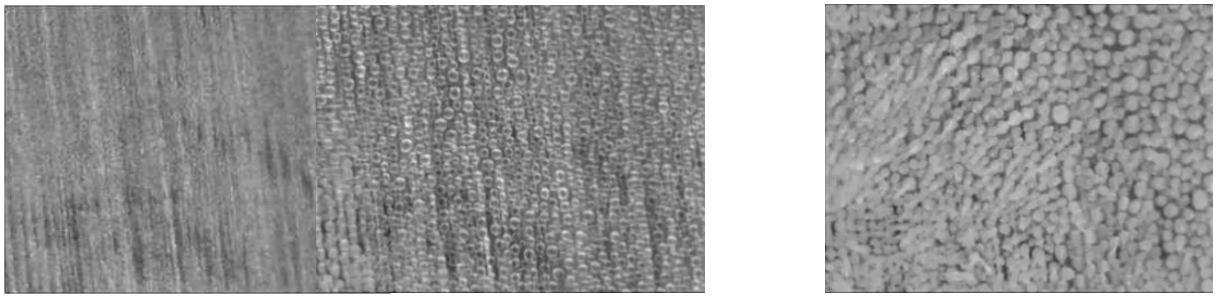


Fig. 10. Frost Formation Area (No.3)

Area of Lower side of frost layer tends to grow higher than the other side. It's just because lower test side has a convex at the leading section that is collided by high humidity air.

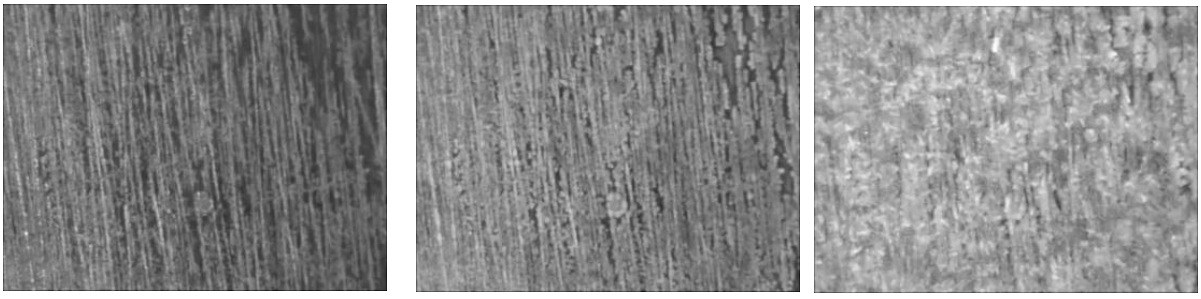
3.2. Observation of Frost Crystals Growth

By changing the one side of the aluminium plate to acrylic plate, the test section was visualized. After frost crystals appear, the interval distance and diameter distance were measured. Fig. 11 and Fig. 12 show the series of picture indicating frost crystal growth process stage.



(a) 60sec (b) 120sec (c)240sec

Fig. 11. Frost growth (No.2)



(a) 0sec (b) 30sec (c) 90sec

Fig. 12. Frost growth (No.3)

Note that the airflow moves from left to right in these pictures. In case of test section No2, condensate droplets coalesce with surrounding and frost crystals are formed on the droplet. In case of test piece No3, coalescence of droplets do not occur. In any test section, frost crystals grow toward the windward.

Next, using the image processing as well as the frost layer area measurement, frost column diameter and the

frost crystal intervals are measured. When the frost crystals generate, these are measured based on the pitch between the distances of the droplets. Measured data are shown in the table below.

Table 3. Various amounts of initial frost crystals forming

	Initial crystal column diameter (mm)	Crystal column interval (mm)	Initial air speed (m/s)	Crystal column appearance (s)
No.1	0.023	0.075	4.34	80
No.2	0.024	0.076	3.10	160
No.3	0.016	0.056	7.23	35

These three initial air speed are different, because height of convexity portion are also different.The larger the initial air flow velocity is, the smaller the crystal column diameter and the crystal distance are. According to the result, it is confirmed that there is a change of frost development process by the difference in the initial velocity of air flow.

3.3. Frost Layer Growth Analysis of Convexo-Concave Plate

First, we verified an analytical model of the frost layer growth in parallel plate. Growth process of frost layer is classified into "crystal growth stage", "frost layer growth stage", and "frost layer full growth stage". Since the melting at frost layer surface was not observed in this experiment, we examined a process until the frost layer growth period.

< Crystal Growth Stage >

In the crystal growth stage, needle-like crystals generates. These are growing one-dimensionally in a direction perpendicular to the cooling surface, porosity forms a large surface rough ness is also rough frost layer. In this study, we used the model of Yamashita[6] et al. that is improved the model of Tao[4-5] et al.

$$(\delta L_f/\delta t) = C_2 \times (h_D / \rho_I) \times (X_a - X_{fs}) \quad (1)$$

$$(\delta d/\delta t) = C_3 \times 2 \times (h_D / \rho_I) \times (X_\gamma - X_I) \quad (2)$$

$$T_\gamma = k_\alpha \times T_\alpha + (1 - k_\alpha) \times T_w \quad (3)$$

$$\rho_f = \frac{\int_0^{Lf} [\frac{\pi}{4} d^2 \rho_I + (l^2 - \frac{\pi}{4} d^2) \times \rho_a] \times dz}{l^2 \times Lf} \quad (4)$$

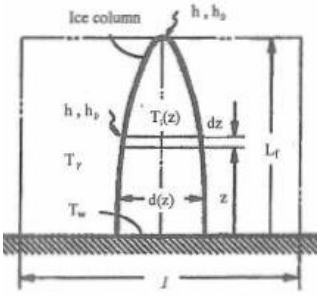


Fig. 13. Model of Tao et al

h_D = Mass Transfer Coefficient [kg / m^2 s ΔX] , X_{fs} = Absolute Humidity of Frost Layer Surface [kg / kg´]
X_f = Absolute Humidity of Frost Layer [kg / kg´], k_a・C_2・C_3:Factor , X_a = Absolute Humidity of Air [kg /kg´]
d = Crystal Diameter [m] , X_l = Absolute Humidity Crystal Column [kg / kg´]
[kg / kg´]=[Amount of water vapor of moist air/ Amount of water vapor of dry air]

Analysis condition

Air in the vicinity of frost is a saturated state (i.e. 100% relative humidity)

Analysis method

(A) Density of ice is calculated using the formula of Fukusako[7] et al (1996) from the cooling surface temperature.

$$\rho_1 = 917 \times (1 - 1.17) \times 10^{-4} \times t_f \quad (5)$$

t_f =Frost Layer Temperature [degC]

(B) Calculating T_γ by using eq. 3. Here, k_α=0.4.

(C) The increasing rate of frost layer height and icicles diameter after ⊿t seconds are calculated by eq. 1 and 2.

(D) Put forward ⊿t seconds, make the frost layer height and the icicle diameter increase each increment. The above process is repeated until convergence.

<Frost layer growth stage>

In the frost layer growth period, side branch generates on the crystal column, and it grows in three dimensionally, therefore the void of frost layer is disappeared, and the surface roughness of the frost layer is reduced and flat frost layer is formed. Roll of vapour is divided into a component to increase the height of the frost layer and increasing the frost layer density.

Analysis condition

(A) Air of the frost layer surface and cooling surface are saturated state (i.e. 100% relative humidity).
(B) Density distribution of frost layer is constant.

Analysis method

(A) Calculate density of ice by using eq (5).
(B) Calculate porosity.
(C) Calculate tortuosity and the effective diffusion coefficient shown in Table 4, Le Gall et al[8].
(D) Calculate surface temperature of frost layer and the saturated vapour pressure corresponding to the cooling surface temperature.
(E) Calculate the mass flux diffusing into frost layer. Here, the saturated vapour pressure is determined from the atmospheric pressure and the absolute humidity by using eq (6).
(F) Calculate the mass flux by using increment of the frost height.
(G) Calculate the increased amount of frost layer density after Δt seconds.
(H) After Δt seconds passed, and considering the increment of frost height, calculation is repeated until the end time.

$$P_v = P_a \frac{X}{0.622 + X} \tag{6}$$

Table 4. The suggested Formulas of Tortuosity

Year	Name	Tortuosity
1969	Brian et al	τ=1.1
1986	Auracheret al	τ=1-0.58×(1-ε)
1993	Taoet al	τ=1/1.1
1997	Le Gall et al	$\tau = \frac{\varepsilon}{\frac{\varepsilon}{1-0.58\times(1-\varepsilon)} + F\times 10\times(1-\varepsilon)\times\varepsilon^{10}}$
2002	Mezedure et al	$\tau = \frac{\varepsilon}{1-(1-\varepsilon)^{0.5}}$

<Transition stage from nascent of frost layer growth period>

Analysis on frost crystal growth and frost layer growth period mentioned above, however, these phenomena are not independent, therefore it should be analyzed continuously. Since the convex-concave plate has a gradient of the frost layer height from upstream to downstream, the transition to frost crystal growth occurs first in the upstream, and also occurs sequentially in the downstream. Period from the start of transition at the upstream to the end of transition at the downstream is defined as transition region. Therefore, transition start point is determined at which the frost height is about 0.10mm, and transition end point is a point that it became 80% of the passage blockage time. By using assumption which the transition is proportional from the start to the end in the transition period, calculations were conducted.

<The results of analysis>Ice column interval and initial ice column diameter is set as initial value referred to experimental result in Table 3 .Table 5 shows the value used in calculation, and Fig. 17 and Fig. 18 show the calculation results of frost layer density and height, respectively.

Table 5 . Calculation Parameter

No.	Transition Region	Frost Nascent Phase	Frost Layer Growth Phase

	Starting Time	Closing Time	Initial Crystal Column Diameter	Crystal Column Interval	Mass Transfer Coefficient	Tortuosity
1	60s	1170s	0.020mm	0.073mm	52g/m^{2}s Δ X	Le Gall et al eq.(F=1)
2	70s	1350s	0.021mm	0.085mm	36g/m^{2}s Δ X	Le Gall et al eq.(F=1)
3	30s	440s	0.012mm	0.065mm	65g/m^{2}s Δ X	Le Gall et al eq.(F=1)

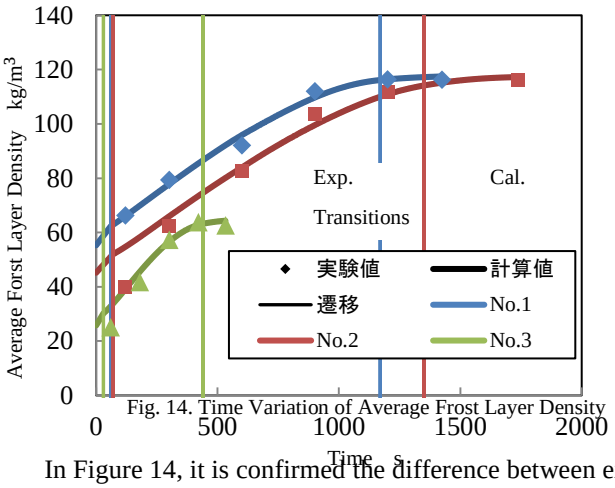


Fig. 14. Time Variation of Average Frost Layer Density

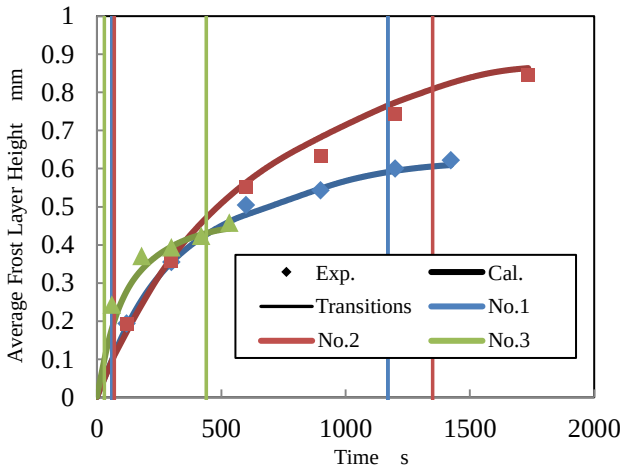


Fig. 15. Time Variation of Average Frost Layer Height

In Figure 14, it is confirmed the difference between experimental value and calculated value in frost nascent are large. Therefore, it is necessary to improve accuracy of the analysis model of this stage.

Figure 16 and Figure 17 show the error band of frost layer density and frost layer height, respectively. Table 6 shows the average error rate.

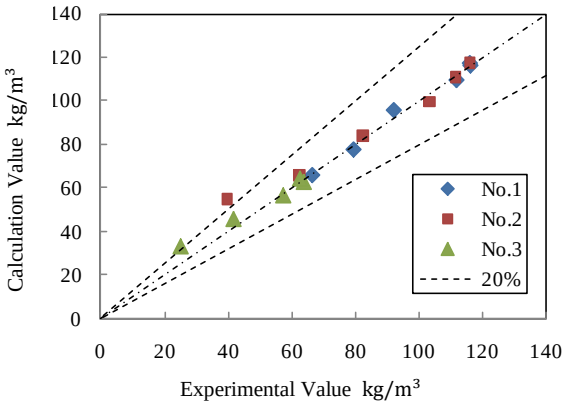


Fig. 16. Error Band of Frost Layer Density

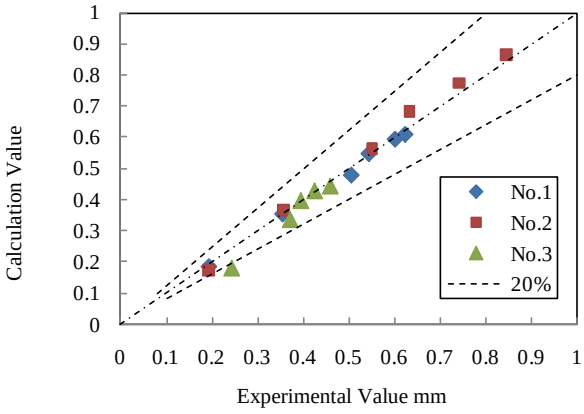


Fig. 17. Error Band of Frost Layer Height

Table 6. Average Error Band

	No.1	No.2	No.3
Ave. Frost Density	1.61%	6.69%	7.48%
Ave. Frost Height	2.33%	4.86%	10.1%

From Figures 16,17, the error band of calculated value is about 10%. Particularly, the average error band is about 2% in No.1.

3.4. Frost Layer Growth Simulation Model of Convexo-Concave Plate

Frost layer growth prediction is based on analysis of 3.3. The simulation refers to crystal column diameter and interval distance that are measured. Because the error rate of No.1 is smallest, it is selected.

Analysis condition

(A) Air of the frost layer surface and cooling surface are saturated state (i.e. 100% relative humidity).
(B) Frost layer density is constant.
(C)Average temperature of frost layer is assumed at surface temperature of frost layer and cooling surface temperature

Analysis method

(A) Calculate Nusselt number by using eq.(7) and eq.(8). And calculate Sherwood number by using eq.(9). Here, $k_{sh} = 0.09$.
(B) Calculate surface temperature of frost layer by using eq.(10) and eq.(11).
(C) Make a calculation about frost crystal growth by following model of Tao[4-5] et al.
(D) When average frost layer height exceeds boundary conditions, make calculation as a transition period.

$$Nu = 0.40\ Re^{1.27}\ Pr^{1/3} \quad (Re < 885) \tag{7}$$
$$Nu = 9.06 \cdot 10^{8}\ Re^{-1.9}\ Pr^{1/3} \quad (Re > 885) \tag{8}$$
$$Nu / Sh = (1 / k_{sh}) \cdot (Pr / Sc)^{1/3} \tag{9}$$
$$Q_a = A_f \cdot \{h_f \cdot (T_a - T_{fs}) + h_{Df} \cdot \gamma \cdot (X_a - X_{fs})\} \tag{10}$$

Q_a: Quantity of Heat Transferred from Air to Frost Layer Surface
h_f: Heat Transfer Coefficient, h_{df}: Mass Transfer Coefficient kg/m^{2}sΔX ,
γ : Latent Heat of Submission J/kg

$$Q_f = A_f \cdot \lambda_f / L_f \cdot (T_{fs} - T_w) \tag{11}$$

Q_f : Quantity of Heat Transferred from Air to Frost Layer to Cooling Surface

$$\dot{m} = h_{Df} \times (X_a - X_{fs}) \tag{12}$$

$\dot{m}$: Frost Formation Flux kg/m^{2}s

Figure 18 to Figure 21 show the calculation results of frost weight, frost layer density, height of frost layer, surface temperature of frost layer, respectively. Table 7 shows the average error bond.

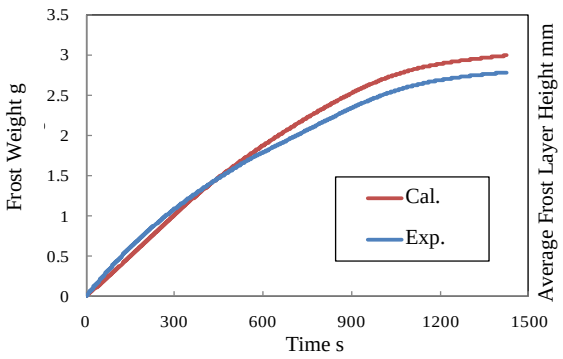


Fig. 18. Frost Weight

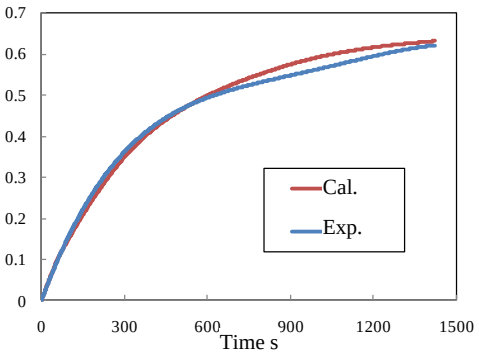
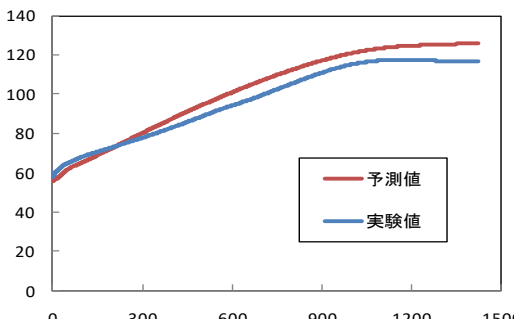
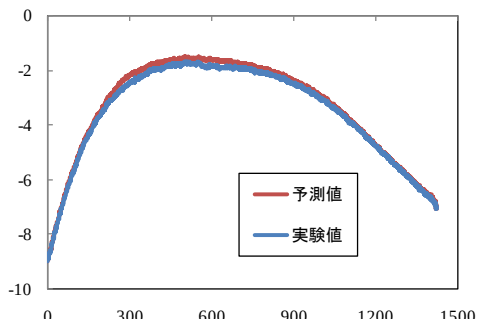


Fig. 19. Average Frost Layer Height





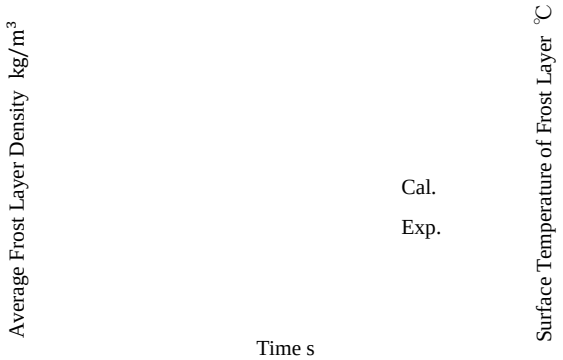


Fig. 20. Average Frost Layer Density

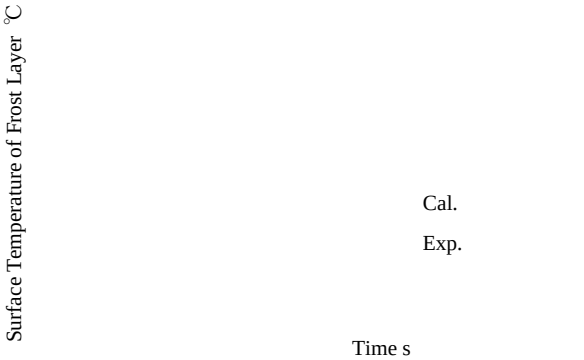


Fig. 21. Surface Temperature of Frost Layer

Table 7. Average error bond

Frost weight	Average frost layer height	Average frost layer density	Surface temperature of frost layer
8.7%	3.4%	5.6%	5.8%

4. CONCLUSION

1. From the frost layer observation, an initial ice column diameter and an ice column interval are specified and it is confirmed that the effect of flow passage geometry on the ice column growth.
2. Previous proposed analytical model for frost layer growth is used for frost density and height prediction. By using the experimentally specified initial ice column value, the estimated value can predict with accuracy within 10% error to compare with experimental result.
3. The calculated result using prediction model for frost layer growth, the frost weight, frost layer density, frost layer height and surface temperature of frost layer are estimated less than 10% error to compare with experimental value.

5. REFERENCE

[1] Adachi T, Mizushima J. 1998, The transfer to the stability and the turbulent flow of a flow in rectangular tube. *RIMS Kokyuroku published*. 1051: p. 202-214.

[2] Adachi T, Uehara H. 2000, Pressure Drop and Heat Transfer Characteristics of Flow in Channels with Periodically Grooved Parts, *Transactions of the JSME*. B67(657).

[3] Yang D. 2006, Frost formation on a cold surface under turbulent flow, *International Journal of Refrigeration*. 29(2): p. 164-169.

[4] Tao Y, Besant R, Mao Y. 1993, Characteristics of frost growth on a flat plate during the early growth period. *ASHRAE Transactions*. 99: p. 746-753.

[5] Tao Y, Besant R, Mao Y. 1994, Frost growth characteristics on heat exchanger surface : measurement and simulation. *HTD*, 286: p. 29-38.

[6] Yamashita K. 2009, Frosting phenomenon in low temperature environments. *Doctor's degree of Tamagawa University*.

[7] Fukusako S, Inaba H. 1996, *Heat transfer phenomenon under the cool temperature environment and applicability*. Yokendo, Tokyo, 14 p.

[8] Le Gall, J.M. Grillot and C. Jallut, "Modelling of Frost Growth and Densification",Int. J. of Heat Mass Transfer. 28,(7) (1997),3177-3187

© 2017 Stichting HPC 2017.
Selection and/or peer-review under responsibility of the organizers of the 12th IEA Heat Pump Conference 2017.